Continuous Dynamical Decoupling with Bounded Controls

Pochung Chen
Department of Physics, National Tsing-Hua University, Hsinchu 100, Taiwan
(Dated: February 1, 2008)

We develop a theory of continuous decoupling with bounded controls from a geometric perspective. Continuous decoupling with bounded controls can accomplish the same decoupling effect as the bang-bang control while using realistic control resources and it is robust against systematic implementation errors. We show that the decoupling condition within this framework is equivalent to average out error vectors whose trajectories are determined by the control Hamiltonian. The decoupling pulses can be intuitively designed once the structure function of the corresponding $SU(n)$ is known and is represented from the geometric perspective. Several examples are given to illustrate the basic idea. From the physical implementation point of view we argue that the efficiency of the decoupling is determined not by the order of the decoupling group but by the minimal time required to finish a decoupling cycle.

I. INTRODUCTION

Quantum decoherence control has been studied intensively in recent years due to the fact that it represents one of the main obstacles in implementing quantum computation. However the problem of decoherence remains daunting. Although there have been rapid advances in physical realization of quantum operations on few levels system in which a single qubit or few qubit can be embedded . The fidelity for those quantum operations, such as Rabi rotation, is typically far below the threshold to make the system scalable. To increase the fidelity, many strategies are proposed to counteract the undesired effects resulting from decoherence. Those strategies can be roughly divided into two categories, depended on if an encoding scheme is used. Some prominent examples in which encoding is needed are the quantum error-correction codes (QECC)[1, 2, 3] and the decoherence-free subspace (DFS).[4, 5, 6] One of the main drawback of the encoding strategies is the large amount of ancillary space needed, especially when the qubit is still a rare resource. As a result, strategies which do not need ancillary systems is highly desirable. Closed-loop decoherence control (such as quantum feedback control [7, 8, 9]) and open-loop decoherence control (such as bang-bang or dynamical decoupling [10, 11, 12, 13]) fall into this category. The open-loop decoherence control typically requires only a limited, *a priori*, knowledge of the system-environment dynamics. Empirical determination of control parameters via quantum tomography has also been proposed recently.[14] In this work we will focus on the dynamical decoupling, but it is acknowledged that no single strategy can efficiently eliminated the problem of decoherence at all levels. Combining or concatenating different strategies is usually necessary for any real physical system.

In the original bang-bang decoupling framework, arbitrarily strong and instantaneous control pulses are utilized to induce frequent unitary interruptions during the evolution of the system. The control Hamiltonian is independent of the system dynamics and are judicially designed to realize an effective decoupling between the system and the environment. The stringent requirement on the control Hamiltonian represents a drawback of the bang-bang decoupling. Experimentally it is impossible to implement arbitrarily strong and instantaneous pulses in real physical systems. An ultra strong and fast control pulse will also inevitably induce transitions to higher energy levels which are usually neglected in the analysis of the bang-bang decoupling. Theoretically is difficulty to describe the evolution with and without control terms simultaneously. This also make it difficult to estimate the robustness of the control and to estimate the error induced by operational imperfections. The highly abstract group theory which is frequently used in the decoupling analysis also make it less intuitive and difficult to make transparent connection to the realization of bang-bang decoupling. To alleviate the need for strong and impulsive control actions, a dynamical decoupling using only bounded-strength Hamiltonian is recently proposed.[15] Within this framework the same group symmetrization is achieved by exploiting the *Eulerian cycles on a Cayley graph of* $\mathcal{G}$,[16] where $\mathcal{G}$ is the decoupling group. On the other hand a complimentary, geometric perspective of bang-bang decoupling is recently proposed to provide a more intuitive picture and provide a method to estimate implementation errors.[14, 17] In this work we extend the geometric picture of bang-bang decoupling to the case of continuous decoupling with bounded controls. We show that the decoupling by symmetrization is equivalent to average out error vectors whose trajectories are determined by the control Hamiltonians. The decoupling pulses can be intuitively designed by viewing the effect of control Hamiltonian from a geometric perspective. To avoid confusing we will use the term *bang-bang decoupling* to refer to the typical decoupling scheme originally proposed.[10, 11, 12, 13] The term *Eulerian decoupling* corresponds to the decoupling with bounded Hamiltonian introduced by L. Viola and E. Knill[15], while the term *continuous decoupling* corresponds to the version of continuous decoupling from a geometric picture developed in this work.

The structure of the paper is the following. In Sec. II we review the original bang-bang decoupling, the Eu-

lerian decoupling, and the geometric perspective of the bang-bang decoupling. In Sec. III we introduce the idea of continuous dynamical decoupling from a geometric perspective. In Sec. IV several examples are given to illustrate how to construct the decoupling pulses. We summarize in Sec. V.

II. REVIEW

A. Bang-bang decoupling decoupling

In general, dynamical decoupling seeks to eliminate the decoherence of an open quantum system by effectively averaging out the interaction between the system and the bath by introducing some strong periodic control Hamiltonian on the system.[10, 11, 12, 13] Following the standard treatment, the dynamics of an quantum open system is determined by the total Hamiltonian

$$H_0 = H_S \otimes \mathbb{1}_B + \mathbb{1}_S \otimes H_B + H_{SB}, \tag{1}$$

where

$$H_{SB} = \sum_\gamma S_\gamma \otimes B_\gamma \tag{2}$$

represents the system-bath interaction. Now introduce a control Hamiltonian $H_c(t) = H_c(t) \otimes \mathbb{1}_B$ acting on the system alone. Denote $U_c(t)$ the time-evolution operator associated with the control Hamiltonian

$$U_c(t) \equiv Texp\left\{-i\int_0^t duH_c(u)\right\}, \tag{3}$$

where T is the time-ordering operator. In periodic dynamical decoupling one is restricted to the situation where the control field is *cyclic*, i.e., $U_c(t) = U_c(t+T_c)$ for some period T_c. For any state $|\psi(t)\rangle$ and any operator O in Schrödinger picture, the corresponding state $|\hat{\psi}(t)\rangle$ and operator $\hat{O}(t)$ in the interaction representation associated with $H_c(t)$ are:

$$|\hat{\psi}(t)\rangle = U_c^\dagger(t)|\psi(t)\rangle = U_c^\dagger(t)U(t)|\psi(0)\rangle, \tag{4}$$

and

$$\hat{O}(t) = U_c^\dagger(t)OU_c(t), \tag{5}$$

where $U(t) = Texp\{-iHt\}$ is the time-evolution operator associated with $H = H_0 + H_c$. It is easy to show that

$$|\hat{\psi}(t)\rangle = Texp\left\{-i\int_0^t du\hat{H}_0(u)\right\}|\psi(0)\rangle, \tag{6}$$

where $\hat{H}_0(t) = U_c^\dagger(t)H_0U_c(t)$. Using the periodic condition $U_c(T_c) = \mathbb{1}_S$ one finds

$$|\psi(T_c)\rangle = U(T_c)|\psi(0)\rangle = U_c^\dagger(T_c)U(T_c)|\psi(0)\rangle = |\hat{\psi}(T_c)\rangle. \tag{7}$$

The *stroboscopic* dynamics at $T_N = NT_c$ for integer N is hence determined by the time evolution operator

$$\hat{U}(T_c) \equiv Texp\left\{-i\int_0^{T_c} du\hat{H}_0(u)\right\}. \tag{8}$$

It is possible to define a k-th order average Hamiltonian $\bar{H}^k$ by applying the Magnus expansion[18] to $\hat{U}(T_c)$, results in

$$\hat{U}(T_c) = e^{-i\left[\bar{H}^0+\bar{H}^1+\ldots\right]T_c}. \tag{9}$$

In particular we have

$$\bar{H}^0 = \frac{1}{T_c}\int_0^{T_c} du\hat{H}_0(u) = \frac{1}{T_c}\int_0^{T_c} duU_c^\dagger(u)H_0(u)U_c(u), \tag{10}$$

and

$$\bar{H}^1 = -\frac{i}{T_c}\int_0^{T_c} dv\int_0^v du\left[\hat{H}_0(v), \hat{H}_0(u)\right]. \tag{11}$$

Higher-order corrections can also be systematically evaluated. In the limit of $T_c \to 0$, which is the ideal limit of bang-bang decoupling, $\bar{H}^0$ becomes the dominant term. It can be viewed as an effective Hamiltonian governing the stroboscopic dynamics under control Hamiltonian. In the following we will focus on designing the effective Hamiltonian $\bar{H}^0$.

Denote $\mathcal{H}_S$ the finite-dimensional state space associated with the system. The idea of decoupling by symmetrization is to identify a discrete decoupling group $\mathcal{G} = \{g_j\}$, $j = \{0, \ldots, |\mathcal{G}| - 1\}$, acting on $\mathcal{H}_S$ via a faithful, unitary, projective representation μ such that $\mu(\mathcal{G}) \subset \mathcal{U}(\mathcal{H}_S)$, the unitary matrices acting on $\mathcal{H}_S$. The bang-bang decoupling via $\mathcal{G}$ is implemented by assigning

$$U_c((l-1)\Delta t + s) = \mu(g_l), s \in [0, \Delta t), \tag{12}$$

with $T_c = |\mathcal{G}|\Delta t$, and $l = \{0, \ldots, |\mathcal{G}| - 1\}$. With this assignment the effective Hamiltonian $\bar{H}^0$ becomes:

$$\bar{H}^0 = \sum_\gamma \bar{S}_\gamma \otimes B_\gamma, \tag{13}$$

where

$$\bar{S}_\gamma \equiv \Pi_{\mathcal{G}}(S_\gamma) = \frac{1}{|\mathcal{G}|}\sum_{g_j \in \mathcal{G}} \mu(g_j)^\dagger S_\gamma \mu(g_j). \tag{14}$$

The nontrivial work is to identify the group $\mathcal{G}$ such that for all γ the effective error operator $\bar{S}_\gamma = \lambda_\gamma \mathbb{1}_S$ where λ_γ is a real number. Once this is accomplished then the effective Hamiltonian $\bar{H}^0$ is reduced to

$$\bar{H}^0 = \mathbb{1}_S \otimes \sum_\gamma \lambda_\gamma B_\gamma. \tag{15}$$

As a result the system is effectively decoupled from the bath, or equivalently the decoherence is suppressed. Note

that in this formulation the underlying control Hamiltonian is never explicitly mentioned. An instantaneous, arbitrary strong control Hamiltonian is needed to implement the desired $U_c(t)$. However, physically it is impossible to implement such an instantaneous control pulse. An arbitrary strong control Hamiltonian would also inevitably induce transition to higher energy states which are neglected when a two level approximation is used to describe the qubit space. Those unphysical requirements represent some of the main drawbacks of the original bang-bang decoupling framework.

B. Eulerian decoupling

In order to alleviate the unphysical requirements of the original bang-bang decoupling framework, L. Viola and E. Knill propose a general framework in which the same group symmetrization can be achieved while using only bounded control Hamiltonians.[15] Physically it uses only bounded control Hamiltonians to steer the time evolution operator. Mathematically it exploits the Eulerian cycles on a Cayley graph[16] of the decoupling group $\mathcal{G}$. Given a decoupling group $\mathcal{G}$, the first step in implementing Eulerian decoupling is to find a generating set $\mathcal{F} = \{f_\alpha\}, \alpha = 1, \ldots, |\mathcal{F}|$, for the decoupling group $\mathcal{G}$. The physical implementation requirement is the ability to generate f_α by some control Hamiltonian $h_\alpha(t)$ over a period of time Δt,

$$f_\alpha = Texp\left\{-i\int_0^{\Delta t} duh_\alpha(u)\right\}, \alpha = 1, \ldots, |\mathcal{F}|. \quad (16)$$

If we image each group element $g_i \in \mathcal{G}$ as a vertex, then f_α can be imaged as the directional, colored edge connecting the vertices. If $g' = f_\alpha g$, then we draw a line from point g to pint g' with color α. An Eulerian cycle is defined as a cycle that uses each edge exactly once. In this case, one can show that it is always possible to find Eulerian cycle, having length $L = |\mathcal{G}||\mathcal{F}|$. [16] A well-defined Eulerian cycle beginning at the identity g_0 of $\mathcal{G}$ can be uniquely specified by the sequence of the edge colors used, $P_E = (p_1, p_2, \ldots, p_L)$, where $p_l \in \mathcal{F}$. An Eulerian decoupling is then implemented by letting $T_c = L\Delta t$ and by assigning $U_c(t)$ as follows:

$$U_c(t)[(l-1)\Delta t + s] = u_l(s)U_c[(l-1)\Delta t], \quad (17)$$

where $s \in [0, \Delta t)$, and $u_l(s) = Texp\{-i\int_0^s duh_l(u)\}$, $u_l(\Delta t) = \mu(p_l)$. In this way the average Hamiltonian $\bar{H}^0$ becomes:

$$\bar{H}^0 = \sum_\gamma \bar{S}_\gamma \otimes B_\gamma, \quad (18)$$

where

$$\begin{aligned}\bar{S}_\gamma = & \frac{1}{|\mathcal{F}||\mathcal{G}|\Delta t}\int_0^{|\mathcal{F}||\mathcal{G}|\Delta t} duU_c^\dagger(t)H_0(t)U_c(t) \\ = & \frac{\sum_{g_j\in\mathcal{G}}}{|\mathcal{G}||\mathcal{F}|\Delta t}\mu(g_j)^\dagger\left\{\sum_{\alpha=1}^{|\mathcal{F}|}\int_0^{\Delta t} dtu_\alpha^\dagger(t)S_\gamma u_\alpha(t)\right\}\mu(g_j).\end{aligned}$$

It can be shown that the same decoupling can be achieved through this average.[15] Assuming that Δt remains the same as in the Eulerian decoupling, the length of the Eulerian decoupling is lengthened by a factor of $|\mathcal{F}|$ compared to the bang-bang decoupling. Eulerian decoupling provides a guideline to design the control Hamiltonian if the decoupling group and it's representation is known. However the search for the decoupling group remains a nontrivial work.

C. The geometric perspective of the bang-bang decoupling

Bang-bang decoupling and Eulerian decoupling schemes make heavy use of the abstract group theory. In recent years a complementary geometric perspective is developed to provide a more intuitive picture.[17] The geometric picture of the bang-bang decoupling utilities the Homomorphic mapping between the Lie group $SU(n)$ and $SO(N)$, where $N = n^2 - 1$. Let λ_i, $i = 1, \ldots, N$ be the N traceless, Hermitian generators of $SU(n)$. The generators $\{\lambda_j\}$ satisfy trace-orthogonality,

$$\mathrm{Tr}(\lambda_i\lambda_j) = M\delta_{ij}, \quad (19)$$

where M is a normalization constant. For any group element $U \in SU(n)$, one can define a rotation $R \in SO(N)$ via

$$U^\dagger\lambda_i U = \sum_{j=1}^N R[U]_{ij}\lambda_j. \quad (20)$$

This defines a homomorphism from $SU(n)$ to a subgroup of $SO(N)$.

Without loss of generality, one can re-write H_0 as

$$\begin{aligned} & H_0 \quad (21)\\ = & H_S\otimes\mathbb{1}_B + \mathbb{1}_S\otimes H_B + H_{SB} \\ = & \mathrm{Tr}(H_S)\mathbb{1}_S\otimes\mathbb{1}_B + (H_S - \mathrm{Tr}(H_S)\mathbb{1})\otimes\mathbb{1}_B + \mathbb{1}_S\otimes H_B \\ + & \mathbb{1}_S\otimes\sum_\gamma \mathrm{Tr}(S_\gamma)B_\gamma + \sum_\gamma (S_\gamma - \mathrm{Tr}(S_\gamma))\otimes B_\gamma \\ = & E_0 + \mathbb{1}_s\otimes H_B' + \sum_{\gamma'} S_\gamma'\otimes B_\gamma', \end{aligned}$$

where S_γ' is traceless. Note that the first term $E_0 = \mathrm{Tr}(H_S)$ only gives rise to an overall phase and can be discarded. For simplicity (and without loss of generality) we will write $H_{SB} = \sum_\gamma S_\gamma\otimes B_\gamma$, where S_γ is traceless.

Any traceless system operator $S_\gamma \in SU(n)$ can be expanded in terms of λ_j, yielding:

$$S_\gamma = \sum_i (s_\gamma)_i\lambda_i \equiv \vec{s}_\gamma\cdot\vec{\lambda}, \quad (22)$$

where

$$(s_\gamma)_i = \frac{1}{M}\mathrm{Tr}(\lambda_i S_\gamma). \tag{23}$$

In other word, a traceless system operator can be represented by a N-dimensional vector . Using this result the system-bath Hamiltonian H_{SB} can be written as follows:

$$H_{SB} = \sum_\gamma S_\gamma \otimes B_\gamma = \sum_\gamma \left(\vec{s}_\gamma \cdot \vec{\lambda}\right) \otimes B_\gamma, \tag{24}$$

where $\vec{s}_\gamma$ is a vector of length N. In the following we should refer $\vec{s}_\gamma$ as error vectors. By using error vectors to represent the system-bath Hamiltonian H_{SB}, the decoupling by symmetrization over a group $\mathcal{G}$ with projective representation $\mu(g_i)$ can be viewed as an average over rotated error vectors. Following this line the average Hamiltonian $\bar{H}^0$ becomes

$$\begin{aligned}
\bar{H}^0 &= \sum_\gamma \frac{1}{|\mathcal{G}|}\sum_{g\in\mathcal{G}} \mu(g)^\dagger S_\gamma \mu(g) \otimes B_\gamma \\
&= \sum_\gamma \frac{1}{|\mathcal{G}|}\sum_{g\in\mathcal{G}} \mu(g)^\dagger \sum_i (\vec{s}_\gamma)_i \lambda_i \mu(g) \otimes B_\gamma \\
&= \sum_\gamma \frac{1}{|\mathcal{G}|}\sum_{g\in\mathcal{G}} \sum_{ij} (\vec{s}_\gamma)_i R[\mu(g)]_{ij} \lambda_j \otimes B_\gamma \\
&= \sum_\gamma \sum_j \left\{ \frac{1}{|\mathcal{G}|}\sum_{g\in\mathcal{G}} \sum_i R^\dagger[\mu(g)]_{ji} (\vec{s}_\gamma)_i \right\} \lambda_j \otimes B_\gamma \\
&= \sum_\gamma \left(\vec{s'}_\gamma \cdot \vec{\lambda}\right) \otimes B_\gamma,
\end{aligned} \tag{25}$$

where the average error vector $\vec{s'}_\gamma$ is equal to

$$\vec{s'}_\gamma = \frac{1}{|\mathcal{G}|}\sum_{g\in\mathcal{G}}\sum_i R^\dagger[\mu(g)]_{ji}(\vec{s}_\gamma)_i = \frac{1}{|\mathcal{G}|}\sum_{g\in\mathcal{G}} R^\dagger[\mu(g)]\vec{s}_\gamma. \tag{26}$$

From the geometric perspective the decoupling condition (in case of quantum memory) is equal to require that the average error $\vec{s}_\gamma$ be zero for all γ. Geometrically each term in group symmetrization procedure corresponds to an effective rotation $R^\dagger[\mu(g)] \in O(N)$ on all error vectors. However it is evident that the error vector can be averaged to zero by a set of rotations which do not correspond to the representation of some decoupling group. It is thus intriguing to discuss if a underlying group structure is necessary to achieve dynamical decoupling.

III. CONTINUOUS DECOUPLING FROM A GEOMETRIC PERSPECTIVE

The geometric picture of the bang-bang decoupling is intuitive but it shares the same drawback as the bang-bang decoupling, i.e., the error vector is instantaneously rotated to another vector by some rotation. This drawback can be alleviated if a bounded control Hamiltonian is used to continuously rotate the error vector. We thus seek to formulate a framework for continuous dynamical decoupling from a geometric perspective. Recall that the average Hamiltonian has the following expression

$$\bar{H}^0 = \frac{1}{T_c}\int_0^{T_c} du U_c^\dagger(u) H_0(u) U_c(u) = \sum_\gamma \bar{S}_\gamma \otimes B_\gamma. \tag{27}$$

Now instead of piecewisely mapping $U_c(t)$ into the representation of some decoupling group, one represents the effective system operator $\bar{S}_\gamma$ by its corresponding average error vector $\vec{s'}_\gamma$. The average error vector can be expressed as the time average over the trajectory of the error vector rotated by $R^\dagger[U_c]$:

$$\begin{aligned}
\bar{S}_\gamma &= \frac{1}{T_c}\int_0^{T_c} du U_c^\dagger(u) S_\gamma U_c(u) \\
&= \frac{1}{T_c}\int_0^{T_c} du \sum_i (s_\gamma)_i U_c^\dagger(u)\lambda_i U_c(u) \\
&= \frac{1}{T_c}\int_0^{T_c} du \sum_{ij} (s_\gamma)_i R[U_c(u)]_{ij}\lambda_j \\
&= \sum_j \left\{ \frac{1}{T_c}\int_0^{T_c} du \sum_i R^\dagger[U_c(u)]_{ji}(s_\gamma)_i \right\}\lambda_j \\
&= \vec{s'}_\gamma \cdot \vec{\lambda},
\end{aligned} \tag{28}$$

where

$$(s'_\gamma)_j = \frac{1}{T_c}\int_0^{T_c} du \sum_i R^\dagger[U_c(u)]_{ji}(s_\gamma)_i. \tag{29}$$

Or using vector notation:

$$\vec{s'}_\gamma = \frac{1}{T_c}\int_0^{T_c} du R^\dagger[U_c(u)]\vec{s}_\gamma. \tag{30}$$

The decoupling condition (in case of quantum memory) is to require $\vec{s'}_\gamma = 0$ for all γ. Note that we don't explicitly require that U_c be the representation of some group. In order to make the design of control Hamiltonian easier it is desirable to make a more transparent connection between the decoupling and the control Hamiltonian. First define a time-dependent error vector via

$$\vec{s}\cdot U_c^\dagger(t)\vec{\lambda}U_c(t) \equiv \vec{s}(t)\cdot\vec{\lambda}. \tag{31}$$

The i-th component of $\vec{s}(t)$ can be expressed as

$$s_i(t) = \frac{1}{M}\mathrm{Tr}\left\{\lambda_i \vec{s}\cdot U_c^\dagger(t)\vec{\lambda}U_c(t)\right\}. \tag{32}$$

It is instructive to study the trajectory of $\vec{s}(t)$ when the control Hamiltonian is proportional to one of the generators of $SU(n)$. Assuming that $H_l(t) = a_l(t)\lambda_l$, where

$a_l(t)$ represents the envelope function of the control pulse, one finds

$$\begin{aligned}\frac{d}{dt}Ms_i(t) &= \mathrm{Tr}\left\{\lambda_i i a_l(t)\lambda_l \vec{s}\cdot U_c^\dagger(t)\vec{\lambda}U_c(t)\right\} \\ &+ \mathrm{Tr}\left\{\lambda_i \vec{s}\cdot U_c^\dagger(t)\vec{\lambda}U_c(t)(-ia_l(t))\lambda_l)\right\} \\ &= ia_l(t)\mathrm{Tr}\left\{\lambda_i\left[\lambda_l, \sum_j s_j(t)\lambda_j\right]\right\} \\ &= ia_l(t)\sum_j s_j(t)\mathrm{Tr}\left\{\lambda_i i\sum_k f_{ljk}\lambda_k\right\} \\ &= ia_l(t)\sum_j if_{lji}s_j(t) \equiv -ia_l(t)\left[L_l\right]_{ij}s_j(t),\end{aligned} \tag{33}$$

where we have defined

$$\left[L_l\right]_{ij} = -if_{lji} = +if_{lij}, \tag{34}$$

and f_{ijk} is the structure function of $SU(n)$. From the $O(N)$ point of view, the effect of control Hamiltonian $a_l(t)\lambda_l$ is to induce a rotation with generator L_l and with speed $a_l(t)$. It is thus useful to express L_i in terms of the natural generators of $SO(N)$. The natural generator of $SO(N)$ are antisymmetric Hermitian matrices $L_{\mu\nu}$ where $\mu,\nu = 1,\cdots N$, whose components have the form

$$[L_{\mu\nu}]_{ij} = -i(\delta_{\mu i}\delta_{\nu j} - \delta_{\mu j}\delta_{\nu i}). \tag{35}$$

We will restrict ourself to $\mu < \nu$ as a convention and to avoid double counting. They satisfy the commutation relation

$$\begin{aligned}&[L_{\mu\nu}, L_{\mu'\nu'}] \\ =\ & -i\left(\delta_{\mu\nu'}L_{\nu\mu'} - \delta_{\mu\mu'}L_{\nu\nu'} + \delta_{\nu\nu'}L_{\mu\mu'} - \delta_{\nu\mu'}L_{\mu\nu'}\right),\end{aligned} \tag{36}$$

and the trace orthogonality condition

$$\mathrm{Tr}(L_{\mu\nu}L_{\mu'\nu'}) = M\delta_{\mu\mu'}\delta_{\nu\nu'}. \tag{37}$$

Giving a control Hamiltonian of the form $a_l(t)\lambda_l$, in the geometric picture it corresponds to a time independent rotation generator L_l and an time-dependent envelope function $a_l(t)$ representing the time dependent speed of the rotation. By expressing L_l in terms of the natural generators of $SO(N)$

$$L_l = \sum_{\mu\nu} X_{\mu\nu}L_{\mu\nu}, \tag{38}$$

a compact notation of the form

$$[\lambda_l, \vec{\lambda}] = \left(\sum_{\mu\nu} X_{\mu\nu}L_{\mu\nu}\right)\vec{\lambda} \tag{39}$$

can be used to represent the effect of control Hamiltonian λ_l. For example, for $SU(3) \to SO(8)$ one has

$$[\lambda_3, \vec{\lambda}] = (-L_{12} + L_{45} + L_{76})\,\vec{\lambda}. \tag{40}$$

It immediately leads us to the conclusion that λ_3 can be used to average any vector in the 1-2 plan to zero with appropriate envelope function. In the appendix we explicitly calculate the $[\lambda_l, \vec{\lambda}]$ for $SU(2), SU(3)$, and $SU(4)$. Using the continuous decoupling from a geometric perspective, the design of the decoupling pulse sequences can be outlined as follows: The first step is to find the corresponding error vectors from the system-bath Hamiltonian. The second step is to identify the useful control Hamiltonian λ_l. The third step is to design a proper envelope function $a(t)$ to ensure the average error vector to be zero.

Continuous decoupling is robust against implementation imperfection because a small implementation error on the control Hamiltonian will only result in a small deviation of the average error vectors from their ideal values. The implementation error can be evaluated via the distance between the ideal average error vector and the real average error vectors. Let $\vec{s'}_{\lambda,id}$ be ideal average error vectors resulted from a perfect control Hamiltonian while $\vec{s'}_\lambda$ be the real average error vectors resulted from a imperfect control Hamiltonian. The Euclidean distance between two vectors $d(\vec{s'}_{\lambda,id}, \vec{s'}_\lambda) \equiv \sqrt{(\vec{s'}_{\lambda,id} - \vec{s'}_\lambda)\cdot(\vec{s'}_{\lambda,id} - \vec{s'}_\lambda)}$ can be used to quantify the implementation error.

IV. EXAMPLES

In this section we study several examples which illustrate the basic idea of continuous decoupling from geometric perspective.

A. Single qubit spin-flip decoherence

Consider a single qubit with a single error operator, $\{S_\alpha\} = \{\sigma_z\}$. In geometric picture it corresponds to a single error vector $\vec{s} = (0,0,1)$. Intuitively, performing any 2π rotation in a plan containing the error vector $\vec{s}$ should average the error vector to zero. Using the results in the appendix it is easy to verify that one can choose the control Hamiltonian to be proportional to $\lambda_1(=\sigma_x)$ or $\lambda_2(=\sigma_y)$. From the geometric perspective, this corresponds to rotate the error vector in x-z or y-z plan using $SO(3)$ generator L_{13} or L_{23}. If we were to choose σ_y and assume that $H_c(t) = a(t)\sigma_y$, the time-dependent error vector becomes

$$\vec{s}(t) = e^{-i\int_0^t dua(u)L_{13}}\vec{s}(0) = e^{-iA(t)L_{13}}\vec{s}(0), \tag{41}$$

where $A(t) = \int_0^t dua(u)$. The decoupling condition can be written as

$$\frac{1}{T_c}\int_0^{T_c} due^{-iA(t)L_{13}}\vec{s}(0) = \vec{0}. \tag{42}$$

The decoupling condition can be satisfied very generally by requiring that

$$e^{-iA(T_c/2)L_{13}} = R[\pi, \hat{y}], \tag{43}$$

and

$$A(T_c/2 + t) = \pi + A(t), t = [0, T_c/2), \tag{44}$$

where $R[\pi, \hat{y}]$ represents a π rotation around y-axis.

Geometrically this corresponds to rotate the error vector from $\vec{s}$ to $-\vec{s}$ at some speed controlled by $a(t)$, and rotate it back to $\vec{s}$ with the same speed profile. The first condition ensures that the error vector is steered to $-\vec{s}$ at half time $t = T_c/2$. The second condition ensures that the contribution from the second half cancels exactly the contribution from the first half, resulting in zero average error vector.

It is known that the minimal decoupling group of bang-bang decoupling in this case is the group $Z_2 = \{e, g\}$ where $g^2 = e$. It is also referred as parity kick in the literature. The corresponding representation can be chosen to be either $\{\mu(e) = \mathbb{1}, \mu(g) = \sigma_x\}$ or $\{\mu(e) = \mathbb{1}, \mu(g) = \sigma_y\}$. From the geometric picture the effect of $\mu(g)$ is to rotate error vector $\vec{s}$ instantaneously to $-\vec{s}$, ensuring the average error vector be zero. It is easy to show that a larger group $C_4 = \{e, g^2, g^3, g^3\}$, where $g^4 = e$, can achieve the same decoupling. The corresponding representation is $\{\mu(e) = \mathbb{1}, \mu(g) = r, \mu(g^2) = r^2, \mu(g^2) = r^3\}$ where r is the $\pi/2$ rotation along x-direction. From the geometric picture this corresponds to rotate the error vector by $\pi/2$ at each kick. From the typical bang-bang decoupling point of view larger decoupling group represents a less optimal decoupling scheme since more kicks are needed. On the other hand when viewed as the limiting case of the continuous decoupling, Z_2 bang-bang decoupling corresponds to require a large amplitude $a(t)$ for small t and turn $a(t)$ off once the error vector $\vec{s}$ is steered to $-\vec{s}$. A different $a(t)$ can be similarly designed to reproduce the C_4 bang-bang decoupling. However in any real physical implementation there is a upper limit for the strength of $a(t)$. Hence there is a minimal time needed to finish one continuous decoupling cycle and the ideal limit of bang-bang decoupling is never reached. It is this minimal T_c, not the order of the decoupling group, when compared to the decoherence time, indicates the efficiency of the decoupling scheme.

B. Single qubit full decoherence

Consider next a single qubit with all possible error operators, $\{S_\alpha\} = \{\sigma_x, \sigma_y, \sigma_z\}$. In geometric picture they correspond to three error vectors $\vec{s}_1 = (1, 0, 0)$, $\vec{s}_2 = (0, 1, 0)$, and $\vec{s}_3 = (0, 0, 1)$. Intuitively a 2π rotation in a plan containing both the vectors $\vec{s}_1$ and $\vec{s}_2$ can average both error vectors to zero, but $\vec{s}_3$ will remain unchanged. However it is possible to design a sequence which average all three error vectors to zero. To see how such a pulse sequence can be constructed, first recall that in previous example the vector $\vec{s}_i(t)$ must reach $-\vec{s}_i$ during the decoupling operation. We thus seek to rotate $\vec{s}_i$ to $-\vec{s}_i$ using alternating generators, in hope that the residual errors will cancel each other when a full decoupling cycle is finished. Using this idea it is straightforward to construct and verify that a sequence of π rotations using following generators $\{\lambda_1, \lambda_3, \lambda_1, \lambda_3, \lambda_3, \lambda_1, \lambda_3, \lambda_1\}$ can average all three error vectors to zero. In Fig.1 we plot the trajectories of three error vectors during the decoupling sequence. It is evident from the figure that a judicial envelope function will ensure that all time integrals of error vectors are zero.

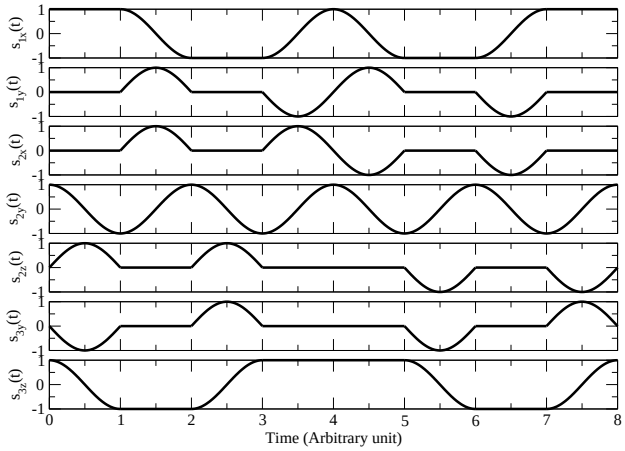

FIG. 1: Trajectories of error vectors under the decoupling sequence described in example B. It is assumed that the envelope function in each sub-period is the same.

The decoupling pulse sequence designed here is equivalent to the Eulerian decoupling prescribed in Ref 15. However as pointed out in previous example the efficiency consideration should be based on the continuous decoupling framework. In Ref 17, an example is given to demonstrate that a decoupling group may not be necessary to achieve the decoupling condition. From the geometric picture of the bang-bang decoupling it suffices to rotate instantaneously the error vectors to the vortices of a tetrahedron. From continuous decoupling point of view it is evident that for this kind of decoupling sequences the residual errors will accumulate when the error vectors are rotated from one vertex to another. It is difficult to cancel these residuals systematically using a design similar to what has been done in this example. Even if it is accomplished, it would represent a less optimal solution. We thus argue that a decoupling group is not necessary to achieve continuous dynamical decoupling but a decoupling group usually provides a guideline to design the optimal continuous decoupling sequence.

C. Two qubits independent decoherence

Next example consists of a two qubit system with independent dephasing error operators. The system-bath Hamiltonian has the form:

$$H_{SB} = g_1 (\sigma_z \otimes \mathbb{1})) \otimes B_1 + g_2 (\mathbb{1} \otimes \sigma_z) \otimes B_2. \quad (45)$$

The Hamiltonian corresponds to two error vectors $\vec{s}_1 = g_1\vec{\lambda}_3$ and $\vec{s}_2 = g_2\vec{\lambda}_6$. Any rotation in $SO(15)$ which can rotate both error vectors by 2π should effectively decouple the system from the dephasing error. In many solid-state qubit, Heisenberg exchange is utilized to implement quantum operations. It is thus advantageous to design a decoupling sequence which is compatible with Heisenberg exchange interaction. In terms of Pauli matrices the Heisenberg interaction is written as

$$H_{ex} = J\sigma_x \otimes \sigma_x + J\sigma_y \otimes \sigma_y + J\sigma_z \otimes \sigma_z. \quad (46)$$

In other words the Heisenberg interaction corresponds to three vectors $\vec{\lambda}_7$, $\vec{\lambda}_{11}$, and $\vec{\lambda}_{15}$ from the geometric perspective. A decoupling sequence compatible with Heisenberg interaction should average error vectors to zero while leave those three vectors in tact. Using the results in the appendix it is apparent that one should avoid using the generators $\lambda_1 \cdots \lambda_6$, $\lambda_8 \cdots \lambda_9$, and $\lambda_{12} \cdots \lambda_{14}$ which either can't average error vectors to zero or have undesirable side effects on Heisenberg interaction. This leaves us to the only choice of λ_7, λ_{11}, and λ_{15}. It is then easy to verify that any one of those three generators can be used as the control Hamiltonian to average out the dephasing error with an appropriately designed envelope function $a(t)$ while leaves the Heisenberg interaction in tact.

D. One qubit with one ancilla level

Our final example consists of a three level system in which the first two levels $|1\rangle, |2\rangle$ are used as the qubit space while the third level $|3\rangle$ is used as an ancilla level used to implement quantum operation in qubit space. We assume that all three levels are coupled to the environment, with the following system-bath Hamiltonian:

$$\begin{aligned} H_{SB} &= g_1 (|1\rangle\langle 1| - |2\rangle\langle 2|) \otimes B_1 \quad (47) \\ &+ g_2 (|1\rangle\langle 3| + |3\rangle\langle 1|) \otimes B_2 + g_3 (|2\rangle\langle 3| + |3\rangle\langle 2|) \otimes B_3. \end{aligned}$$

This system-bath Hamiltonian corresponds to three error vectors $\vec{s}_1 = \vec{\lambda_3}$, $\vec{s}_2 = \vec{\lambda_4}$, and $\vec{s}_3 = \vec{\lambda_6}$. By consulting the $SU(2) \to SO(8)$ mapping in the appendix it is easy to show that all three error vectors can be averaged to zero via the generator λ_2. This simple example illustrates that the continuous dynamical decoupling from geometric perspective can be straightforwardly applied not only to the logical qubit space but also the physical qubit space or the larger space in which the physical qubit space is embedded in.

V. SUMMARY AND DISCUSSION

In summary we have developed a continuous dynamical decoupling framework from a geometric perspective. Within this framework, the need to perform unphysical, arbitrarily strong and fast control is eliminated, and bang-bang control can be viewed as a unphysical limit of the continuous decoupling in which the control Hamiltonian is unbounded. The decoupling condition is equal to require that all time-dependent error vectors $\vec{s}_\gamma$ average to zero at the end of the decoupling cycle. The trajectories of the error vectors are steered by the control Hamiltonian. By expressing control Hamiltonian in terms of the generators of $SU(n)$, the geometric picture provides an intuitive way to design the decoupling pulse sequences, provided that the structure function of the corresponding $SU(n)$ is known. Several examples are given to explicitly illustrate how to design the decoupling sequences starting from a given system-bath Hamiltonian. We also show that, in stead of the order of the decoupling group, the minimal time needed to finish one continuous decoupling cycle. The framework is not restricted to physical qubit space or logical qubit space. The ancilla levels or other relevant nearby levels can be naturally included in the analysis. This is important especially when ancilla levels are needed to perform quantum operation or when the nearby levels can not be neglected.

The paper has focused on designing the decoupling pulses which are ideal for quantum memory. Less is addressed about how to perform quantum operation and decoupling at the same time. The continuous decoupling framework developed in this work can be extended to systematically treat this problem.[14]. The detail of the analysis is beyond the scope of this work and will be presented elsewhere. It is also intriguing to discuss the issue of optimal control. In a typical bang-bang decoupling framework a decoupling group is identified, assuming that the corresponding time evolution operators can be implemented. However in real system the possible control Hamiltonian at our disposal might be limited and the desired time evolution operators might not be achievable. It is thus nature to ask the complementary questions: Giving a set of possible control Hamiltonian, what is the optimal decoupling sequence? The geometric continuous decoupling framework developed here is suitable to answer this question. As a simplest example consider the case where some of the generators of $SU(n)$ can not be used as the control Hamiltonian. In this case one can use the remaining generators and their corresponding rotations to construct a (sub)-optimal decoupling sequence.

Recently there has been efforts to unify the dynamical decoupling and the quantum Zeno effect.[19] Roughly speaking bang-bang control and quantum Zero effect both require a strong interaction with a quantum system. This idea shared by two scheme leads to the possible unification. It is thus very interesting to see if the continuous decoupling scheme in which the arbitrarily strong pulses

are not necessary can still be connected to the quantum Zeno effect.

APPENDIX: $SU(n)$ AND $SO(N)$

In this appendix we explicitly calculate the correspondence between the generators of $SU(n)$ and the natural generators of $SO(N)$ where $N = n^2 - 1$ using the procedure outlined in Sec III. We adapt the following convention for the natural generators of $SO(N)$:

$$[L_{\mu\nu}]_{ij} = -i(\delta_{\mu i}\delta_{\nu j} - \delta_{\mu j}\delta_{\nu i}), \tag{A.1}$$

where $\mu < \nu$. Note that the choise of the generators of $SU(n)$ is not unique. Unitary transformation on a set of generators results in another set of generators. However this only amounts to an rotation on error vectors and the basis vectors of $SO(N)$.

1. $SU(2)$ and $SO(3)$

Let $\lambda_1 = \sigma_x$, $\lambda_2 = \sigma_y$, and $\lambda_3 = \sigma_z$ be the 3 generators of $SU(2)$. They satisfy the trace-orthogonality

$$\mathrm{Tr}(\lambda_i\lambda_j) = 2\delta ij. \tag{A.2}$$

It is easy to verify that

$$[\lambda_1, \vec{\lambda}] = +4L_{23}\vec{\lambda}, \tag{A.3}$$
$$[\lambda_2, \vec{\lambda}] = -4L_{13}\vec{\lambda}, \tag{A.4}$$
$$[\lambda_3, \vec{\lambda}] = +4L_{12}\vec{\lambda}. \tag{A.5}$$

2. $SU(3)$ and $SO(8)$

A standard set of generators of the $SU(3)$ are the Gell-Mann matrices:

$$\lambda_1 = \begin{pmatrix} 0 & 1 & 0 \\ 1 & 0 & 0 \\ 0 & 0 & 0 \end{pmatrix}, \lambda_2 = \begin{pmatrix} 0 & -i & 0 \\ i & 0 & 0 \\ 0 & 0 & 0 \end{pmatrix}, \lambda_3 = \begin{pmatrix} 1 & 0 & 0 \\ 0 & -1 & 0 \\ 0 & 0 & 0 \end{pmatrix}, \tag{A.6}$$

$$\lambda_4 = \begin{pmatrix} 0 & 0 & 1 \\ 0 & 0 & 0 \\ 1 & 0 & 0 \end{pmatrix} \lambda_5 = \begin{pmatrix} 0 & 0 & -i \\ 0 & 0 & 0 \\ i & 0 & 0 \end{pmatrix}, \lambda_6 = \begin{pmatrix} 0 & 0 & 0 \\ 0 & 0 & 1 \\ 0 & 1 & 0 \end{pmatrix}, \tag{A.7}$$

$$\lambda_7 = \begin{pmatrix} 0 & 0 & 0 \\ 0 & 0 & -i \\ 0 & i & 0 \end{pmatrix}, \lambda_8 = \frac{1}{\sqrt{3}} \begin{pmatrix} 1 & 0 & 0 \\ 0 & 1 & 0 \\ 0 & 0 & -2 \end{pmatrix}. \tag{A.8}$$

They satisfy the trace-orthogonality

$$\mathrm{Tr}(\lambda_i\lambda_j) = 2\delta ij. \tag{A.9}$$

Using this set of generators one can verify the following relations

$$\begin{aligned}
[\lambda_1, \vec{\lambda}] &= (+4L_{23} + 2L_{47} + 2L_{65})\vec{\lambda}, \\
[\lambda_2, \vec{\lambda}] &= (-4L_{13} + 2L_{46} + 2L_{57})\vec{\lambda}, \\
[\lambda_3, \vec{\lambda}] &= (+4L_{21} + 2L_{45} - 2L_{76})\vec{\lambda}, \\
[\lambda_4, \vec{\lambda}] &= (-2L_{62} - 2L_{71} - 2L_{53} - 2\sqrt{3}L_{58})\vec{\lambda}, \\
[\lambda_5, \vec{\lambda}] &= (+2L_{16} + 2L_{34} - 2L_{72} - 2\sqrt{3}L_{84})\vec{\lambda}, \\
[\lambda_6, \vec{\lambda}] &= (-2L_{24} + 2L_{37} + 2L_{51} + 2\sqrt{3}L_{78})\vec{\lambda}, \\
[\lambda_7, \vec{\lambda}] &= (+2L_{14} + 2L_{25} - 2L_{63} - 2\sqrt{3}L_{86})\vec{\lambda}, \\
[\lambda_8, \vec{\lambda}] &= (+2\sqrt{3}L_{45} + 2\sqrt{3}L_{67})\vec{\lambda}.
\end{aligned} \tag{A.10}$$

3. $SU(4)$ and $SO(15)$

For $SU(n)$ where n is a power of 2, it is convenient to use the product of Pauli matrices to form the generator of $SU(n)$. We hence use the following assignment for the generators of $SU(4)$:

$$\begin{aligned}
&\lambda_1 = \sigma_1 \otimes \mathbb{1}, \lambda_2 = \sigma_2 \otimes \mathbb{1}, \lambda_3 = \sigma_3 \otimes \mathbb{1}, \\
&\lambda_4 = \mathbb{1} \otimes \sigma_1, \lambda_5 = \mathbb{1} \otimes \sigma_2, \lambda_6 = \mathbb{1} \otimes \sigma_3, \\
&\lambda_7 = \sigma_1 \otimes \sigma_1, \lambda_8 = \sigma_1 \otimes \sigma_2, \lambda_9 = \sigma_1 \otimes \sigma_3, \\
&\lambda_{10} = \sigma_2 \otimes \sigma_1, \lambda_{11} = \sigma_2 \otimes \sigma_2, \lambda_{12} = \sigma_2 \otimes \sigma_3, \\
&\lambda_{13} = \sigma_3 \otimes \sigma_1, \lambda_{14} = \sigma_3 \otimes \sigma_2, \lambda_{15} = \sigma_3 \otimes \sigma_3.
\end{aligned} \tag{A.11}$$

(A.12)

The generators satisfy the trace-orthogonality

$$\mathrm{Tr}(\lambda_i\lambda_j) = 4\delta_{ij}. \tag{A.13}$$

By matrix manipulation one can verify that the following relations holds

$$\begin{aligned}
[\lambda_1, \vec{\lambda}] &= (+8L_{2,3} + 8L_{10,13} + 8L_{11,14} + 8L_{12,15})\,\vec{\lambda} \\
[\lambda_2, \vec{\lambda}] &= (-8L_{1,3} - 8L_{7,13} - 8L_{8,14} - 8L_{9,15})\,\vec{\lambda} \\
[\lambda_3, \vec{\lambda}] &= (+8L_{1,2} + 8L_{7,10} + 8L_{8,11} + 8L_{9,12})\,\vec{\lambda} \\
[\lambda_4, \vec{\lambda}] &= (+8L_{5,6} + 8L_{8,9} + 8L_{11,12} + 8L_{14,15})\,\vec{\lambda} \\
[\lambda_5, \vec{\lambda}] &= (-8L_{4,6} - 8L_{7,9} - 8L_{10,12} - 8L_{13,15})\,\vec{\lambda} \\
[\lambda_6, \vec{\lambda}] &= (+8L_{4,5} + 8L_{7,8} + 8L_{10,11} + 8L_{13,14})\,\vec{\lambda} \\
[\lambda_7, \vec{\lambda}] &= (+8L_{2,13} - 8L_{3,10} + 8L_{5,9} - 8L_{6,8})\,\vec{\lambda} \\
[\lambda_8, \vec{\lambda}] &= (-8L_{2,14} - 8L_{3,11} - 8L_{4,9} + 8L_{6,7})\,\vec{\lambda} \\
[\lambda_9, \vec{\lambda}] &= (+8L_{2,15} - 8L_{3,12} + 8L_{4,8} - 8L_{5,7})\,\vec{\lambda} \\
[\lambda_{10}, \vec{\lambda}] &= (-8L_{1,13} + 8L_{3,7} + 8L_{5,12} - 8L_{6,11})\,\vec{\lambda} \\
[\lambda_{11}, \vec{\lambda}] &= (-8L_{1,14} + 8L_{3,8} - 8L_{4,12} + 8L_{6,10})\,\vec{\lambda} \\
[\lambda_{12}, \vec{\lambda}] &= (-8L_{1,15} + 8L_{3,9} + 8L_{4,11} - 8L_{5,10})\,\vec{\lambda} \\
[\lambda_{13}, \vec{\lambda}] &= (+8L_{1,10} - 8L_{2,7} + 8L_{5,15} - 8L_{6,14})\,\vec{\lambda} \\
[\lambda_{14}, \vec{\lambda}] &= (+8L_{1,11} - 8L_{2,8} - 8L_{4,15} + 8L_{6,13})\,\vec{\lambda} \\
[\lambda_{15}, \vec{\lambda}] &= (+8L_{1,12} - 8L_{2,9} + 8L_{4,14} - 8L_{5,13})\,\vec{\lambda}
\end{aligned}$$

ACKNOWLEDGMENTS

We acknowledge the support of National Science Council in Taiwan through grant NSC 93-2112-M-007-038.

---

[1] P. W. Shor, Phys. Rev. A **52**, R2493 (1995).
[2] A. M. Steane, Phys. Rev. Lett. **77**, 793 (1996).
[3] E. Knill and R. Laflamme, Phys. Rev. Lett. **55**, 900 (1997).
[4] P. Zanardi and M. Rasetti, Phys. Rev. Lett. **79**, 3306 (1997).
[5] L.-M. Duan and G.-C. Guo, Phys. Rev. Lett. **79**, 1953 (1997).
[6] D. A. Lidar, I. L. Chuang I. L., and K. B. Whaley, Phys. Rev. Lett. **81**, 2594 (1998).
[7] H. M. Wiseman and G. J. Milburn, Phys. Rev. Lett. **70**, 548 (1992).
[8] A. C. Doherty and K. Jacobs, Phys. Rev. A **60**, 2700 (1999).
[9] C. Ahn, A. C. Doherty, and A. J. Landahl, Phys. Rev. A **65**, 042301 (2002).
[10] L. Viola, E. Knill, and S. Lloyd, Phys. Rev. Lett. **82**, 2417 (1999).
[11] L. Viola, S. Lloyd, and E. Knill, Phys. Rev. Lett. **83**, 4888 (1999).
[12] P. Zanardi, Phys. Lett. A **258**, 77 (1999).
[13] L. Viola, E. Knill, and S. Lloyd, Phys. Rev. Lett. **85**, 3520 (2000).
[14] M. S. Byrd and D. A. Lidar, Phys. Rev. A **67**, 012324 (pages 14) (2003).
[15] L. Viola and E. Knill, Phys. Rev. Lett. **90**, 037901 (2003).
[16] B. Bollobás, *Modern Graph Theory* (Springer-Verlag, 1998).
[17] M. S. Byrd and D. A. Lidar, Quantum Information Processing **1**, 19 (2002).
[18] W. Magnus, Commun. Pure. Appl. Math. **7**, 649 (1954).
[19] P. Facchi, D. A. Lidar, and S. Pascazio, Phys. Rev. A **69**, 032314 (2004).